Application of the Preisach and Jiles–Atherton models to the simulation of hysteresis in soft magnetic alloys

M. Pasquale[a] and G. Bertotti
IEN Galileo Ferraris and INFM, Corso Massimo D'Azeglio 42, 10125 Torino, Italy

D. C. Jiles and Y. Bi
Ames Laboratory, Iowa State University, Ames, Iowa 50011

This article describes the advances in unification of model descriptions of hysteresis in magnetic materials and demonstrates the equivalence of two widely accepted models, the Preisach (PM) and Jiles–Atherton (JA) models. Recently it was shown that starting from general energy relations, the JA equation for a loop branch can be derived from PM. The unified approach is here applied to the interpretation of magnetization measured in nonoriented Si–Fe steels with variable grain size $\langle s \rangle$, and also in as-cast and annealed Fe amorphous alloys. In the case of NO Fe–Si, the modeling parameter k defined by the volume density of pinning centers is such that $k \approx A + B/\langle s \rangle$, where the parameters A and B are related to magnetocrystalline anisotropy and grain texture. The value of k in the amorphous alloys can be used to estimate the microstructural correlation length playing the role of effective grain size in these materials. © *1999 American Institute of Physics.* [S0021-8979(99)23808-X]

I. INTRODUCTION

This article describes the advances in unification of model descriptions of hysteresis in magnetic materials and demonstrates how the equivalence of two widely accepted, apparently disparate models, the Preisach (PM) and Jiles–Atherton (JA) models can be exploited in the analysis of the microstructural features of soft magnetic materials. Recently it was shown that, starting from general energy relations, the JA equation for a saturation loop branch can be derived from PM.[1] In particular the JA equation for the magnetization

$$\frac{dM(H_a)}{dH_a} = \frac{M_{\rm an}(H_a) - M(H_a)}{k - \alpha[M_{\rm an}(H_a) - M(H_a)]} \tag{1}$$

can be obtained from the PM integral

$$M = 2M_s \int_0^{\infty} dh_c \int_0^{b(h_c)} dh_u \, p(h_c, h_u) \tag{2}$$

as a special case in which the Preisach distribution is written as

$$p(h_c, h_u) = \frac{1}{k} \exp(-h_c/k) \frac{dM_{\rm an}}{dh_u}, \tag{3}$$

where $M_{\rm an}$ is the anhysteretic magnetization, k the volume density of pinning centers, and α the mean field parameter. In compliance with the JA approach $M_{\rm an}$ is expressed as

$$M_{\rm an}(H_a) = M_s \left[\coth\left(\frac{H_a}{a}\right) - \frac{a}{H_a} \right], \tag{4}$$

where the parameter a is associated with the domain density. Reversible contributions can be taken into account writing total magnetization as

$$dM = [(1-c)dM_{\rm irr} + c\,dM_{\rm an}] \tag{5}$$

exactly as in the JA model.

In this article, the unified approach is applied to the simulation and interpretation of magnetization curves, symmetric major and minor loops measured in nonoriented Si–Fe steel with variable grain size $\langle s \rangle$ and in $Fe_{78}B_{13}Si_9$ metallic glass, heat treated to achieve different structural conditions. A set of experimental hysteresis loop data is used to perform the identification of modeling parameters valid for both approaches, and the parameters are shown to be related to microstructural features. In the case of nonoriented Fe–Si the parameter k, associated with the average coercive field and the pinning density, is shown to obey a law $k \approx A + B/\langle s \rangle$, where the A and B coefficients can be related to the magnetocrystalline anisotropy and the grain texture. The same parameter k, in the case of $Fe_{78}B_{13}Si_9$, can also be used to estimate the correlation length of dynamic magnetization processes[2,3] which plays the role of an effective grain size. In this metallic glass it is observed that $k \approx k_0 + D/\lambda$, where the parameter D can be connected to the coupling of quenched-in stress and the magnetostriction constant and k_0 is related to hysteresis in absence of stress and to surface conditions. Using the unified approach to hysteresis modeling it is possible to obtain quite satisfactory results at medium and large inductions, but discrepancies between experimental data and modeling predictions can be found at low inductions, around the demagnetized state, where the initial assumptions on the modeling equivalence do not hold. This behavior reflects the different intrinsic characteristics of the JA and PM. These different features are here exploited in a joint effort directed to microstructural analysis, but necessarily imply a finite range of applicability.

[a]Electronic mail: pasquale@ien.it

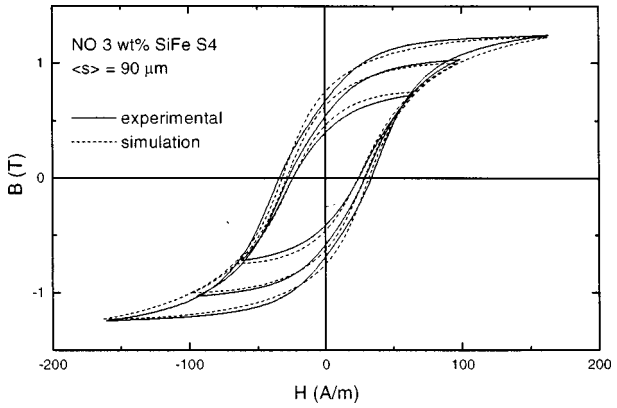

FIG. 1. Comparison between experimental and simulated loop data on the nonoriented 3 wt % SiFe S4 with grain size $\langle s\rangle = 90\ \mu$m. Continuous line experimental data, dotted line JA-PM modeling. Modeling parameters are given in Table I.

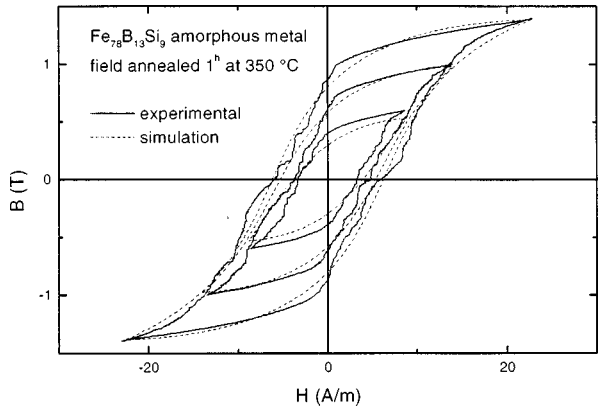

FIG. 2. Comparison between experimental and modeling data on the $Fe_{78}B_{13}Si_9$ metallic glass after annealing for 1 h at 350 °C with a saturating longitudinal applied field. Continuous line experimental data, dotted line JA-PM modeling. Experimental data results noisy due to the small number of domain walls (3-5) moving with a sequence of Barkhausen jumps. Modeling parameters are given in Table II.

II. APPLICATION OF THE JILES–ATHERTON AND PREISACH MODELS

As a working example of how the unified approach can be applied to the analysis of the the microstructural information contained in a set of hysteresis curves, we have collected static hysteresis data on soft crystalline and amorphous materials. The different samples were characterized using a custom built, computer controlled, 14 bit digital Wattmeter hysteresigraph. Symmetric major and minor loops were obtained at frequencies between 0.5 and 10 Hz on the following:

(1) Nonoriented 3 wt % Si–Fe Epstein samples (300 mm×30 mm×350 μm) with variable grain size $\langle s\rangle \approx 55$, 90, 175 μm.
(2) $Fe_{78}B_{13}Si_9$ amorphous ribbon, in the as-cast state and two annealed conditions obtained after 1 and 2 h at 350 °C under longitudinal saturating field (300 mm×5 mm ×20 μm).

All materials were characterized to obtain density and conductivity, together with an evaluation of the surface conditions and the grain size. The comparison of experimental and modeling results was then used in the following sections to establish the connection between relevant modeling parameters and microstructural features. Satisfactory hysteresis modeling results, depicted in Fig. 1 (NO 3 wt % SiFe S3) and Fig. 2 ($Fe_{78}B_{13}Si_9$ annealed 1 h at 350 °C) were obtained using the parameters shown in Tables I and II, respectively.

III. NONORIENTED 3 wt % SiFe

In the case of nonoriented Fe–Si the samples were annealed with different time-temperature combinations (of the order of 1 h at 1000 °C) in order to obtain increasing grain sizes: $\langle s\rangle \approx 55$, 90, 175 μm. The increasing grain size is also associated with better texture and softer magnetic characteristics, leading to a lower coercive field and a higher remanence magnetization.

Through the modeling it is observed that the pinning density (or average coercivity) parameter obeys a simple law

$$k \approx A + B/\langle s\rangle, \tag{6}$$

where the parameters A and B can be related to magnetocrystalline anisotropy and texture.

The parameter k of Table I is related to the overall coercive field of the material, although the precise value of the saturation loop coercivity will in general depend on other details of the distribution as well. Coercivity field models are generally based on the idea that the coercive field is due to the nucleation of some principal domain structure in the individual grains. These models lead to predictions for the coercive field H_c of a polycrystal of the form

$$H_c = H_{\mathrm{AN}}\frac{l_W}{s} + N_{\mathrm{eff}}M_s, \quad H_{\mathrm{AN}} = \frac{2K_1}{\mu_0 M_s}, \quad l_W = \sqrt{\frac{A}{K_1}}, \tag{7}$$

where H_{AN} is the anisotropy field and l_W is the domain wall thickness parameter, dependent on the exchange stiffness A and the anisotropy constant K_1. Equation (7) has exactly the same structure as Eq. (6). The term dependent on the grain size s can be estimated by inserting the typical values of A, K_1, and M_s for silicon–iron alloys. The result is

$$H_{\mathrm{AN}}\frac{l_W}{s} \approx \frac{1000}{s}\ \mathrm{A/m} \tag{8}$$

TABLE I. Modeling parameters referring to nonoriented Epstein frame strips of 3 wt % SiFe 350 μm thick.

Sample	k	α	a	c	I_p	$\langle s\rangle$ (μm)	A	B
NO 3 wt % SiFe S1	60	80	50	0.1	1.6	55		
NO 3 wt % SiFe S4	40	55	40	0.1	1.8	90	8.9	2808
NO 3 wt % SiFe S6	25	40	35	0	1.85	175		

TABLE II. Modeling parameters referring to 20-μm-thick ribbons, width 5 mm, length 300 mm of $Fe_{78}B_{13}Si_9$.

Sample	k	α	a	c	I_p	λ (μm)	k_0	D
$Fe_{78}B_{13}Si_9$ As cast	20	33	13	0.6	0.9	285		
$Fe_{78}B_{13}Si_9$ 1 h 350 °C	8	14	15	0.15	1.38	1000	2.4	5053
$Fe_{78}B_{13}Si_9$ 2 h 350 °C	3	5	5	0.1	1.4	5000		

when s is expressed in μm and the value obtained is of the same order of the value reported in Table I. The term $N_{\text{eff}}M_s$ of Eq. (7) is attributed to magnetostatic effects taking place at the grain boundaries. Therefore, it is expected to be affected by texture effects. The fact that this term is just a constant suggests that the overall texture effect is approximately independent of grain size and may be separated.

IV. Fe BASED AMORPHOUS METALS

In the case of an $Fe_{78}B_{13}Si_9$ amorphous metal the value of k can be used to estimate the structural correlation length playing the role of effective grain size in these materials. In metallic glasses, DW dynamics are strongly connected to the role of quenched-in stress and surface anomalies. Analysis of hysteresis data with PM or the statistical theory of losses[5] leads to the natural definition of a correlation length, active both in static and dynamic conditions. This length λ, is currently under scrutiny in several magnetostrictive amorphous alloys and appears in the relation

$$k = k_0 + \frac{D}{\lambda}, \tag{9}$$

where D appears to be directly proportional to the degree of quenched-in stress and the magnetostriction constant (in this case 4×10^{-5}), the correlation length λ increases by annealing and the constant k_0 represents the contributions to hysteresis after full relaxation, usually related to the surface conditions.[6] It has been shown that the value of D becomes vanishing in the case of zero magnetostriction while the value of λ (Table II) can be related to the domain wall spacing,[3,4,7] since the domain structure in magnetostrictive materials changes from maze-like to very regular after longitudinal field annealing. This initial complex structure is also reflected by a high reversible contribution to magnetization (c parameter) which sharply decreases after heat treatments under longitudinal field, to produce a final state with only a small number (5-3) of longitudinal and regularly spaced domain walls. Referring to Eq. (8) and inserting a value of $K_1 \approx 1000\ \text{J m}^{-3}$ we obtain a value of $D \approx 5000$ for correlation lengths expressed in μm.

V. MINOR LOOPS

The unified modeling procedure used above usually gives satisfactory results at medium and large inductions, as required by the assumptions discussed in Ref. 1. The identification of modeling parameters is strongly dependent on the degree of accuracy required in the reproduction and prediction of minor loop behavior. Identification of parameters implies the minimization of errors in a multidimensional space, requiring some degree of compromise. The intrinsic characteristics of JA, i.e., speed and simplicity and PM, i.e., generality and accuracy are brought to an agreement which can only be partial, due to the respective local and nonlocal memory properties. The data presented so far refers to the conditions where the unified approach is successful, i.e., along saturation loop branches, but discrepancies can be found at low inductions, around the demagnetized state, where the PM shows a higher level of flexibility. These differences are mainly related to the role of reversible magnetization processes at reversal points, where history-dependent properties become predominant.

ACKNOWLEDGMENT

This work was supported by NATO, Division of Scientific Affairs, under Collaborative Research Grant No. CRG 960765.

[1] M. Pasquale, V. Basso, G. Bertotti, D. C. Jiles, and Y. Bi, J. Appl. Phys. **83**, 6497 (1998).
[2] C. Appino, G. Durin, V. Basso, C. Beatrice, M. Pasquale, and G. Bertotti, J. Appl. Phys. (these proceedings).
[3] M. Pasquale, F. Offi, A. Infortuna, E. Ferrara, C. Beatrice, C. Appino, and G. Bertotti, J. Phys. IV **Pr2**, 635 (1998).
[4] G. Bertotti, V. Basso, and G. Durin, J. Appl. Phys. **79**, 5764 (1996).
[5] G. Bertotti, IEEE Trans. Magn. **24**, 621 (1988).
[6] H. Kronmüller, Proc. RQM Sendai, 1981 (unpublished), p. 971.
[7] H. Kronmüller, J. Magn. Magn. Mater. **24**, 159 (1981).